IOPscience iopscience.iop.org

Home Search Collections Journals About Contact us My IOPscience

Morphology dependence of weak-anti-localisation parameters in bismuth films

This article has been downloaded from IOPscience. Please scroll down to see the full text article.

1989 J. Phys.: Condens. Matter 1 6665

(http://iopscience.iop.org/0953-8984/1/37/013)

View the table of contents for this issue, or go to the journal homepage for more

Download details:
IP Address: 171.66.16.96
The article was downloaded on 10/05/2010 at 20:02

Please note that terms and conditions apply.

J. Phys.: Condens. Matter 1 (1989) 6665–6677. Printed in the UK

Morphology dependence of weak-anti-localisation parameters in bismuth films

H White† and D S McLachlan
Department of Physics and Condensed Matter Research Group, University of the Witwatersrand, Johannesburg, Republic of South Africa

Received 7 December 1988

Abstract. The electrical transport properties of polycrystalline bismuth films sputtered onto substrates held at different temperatures have been studied. All the films measured have negative temperature coefficients of resistance between 1.4 and 300 K and lie in the weak-anti-localisation regime below about 15 K. The temperature dependence of the inelastic length for all the films ($T < 15$ K) was extracted from magnetoresistance measurements and is dependent on the distribution of the crystallite orientations which is, in turn, dependent on the substrate temperature during sputtering. Films sputtered onto substrates held at temperatures above room temperature show the characteristic weak localisation and electron–electron interaction temperature dependence, while films sputtered onto substrates held below room temperature show a more complicated temperature dependence at low temperatures in zero field.

1. Introduction

The weakly localised regime has received much attention since 1979, with the characteristic weak-localisation (WL) and associated electron–electron interaction (EEI), temperature T and magnetic field B dependences of the conductivity σ having been studied in a wide range of systems. The microscopic treatment of localisation within the regime where perturbative methods are valid originated from the scaling ideas of Abrahams *et al* (1979), and the work of Gorkov *et al* (1979). The associated EEI processes were first considered by Altshuler and Aronov (1979a, b), Altshuler *et al* (1980a, b) and, independently, Fukuyama (1980). The effects of WL are severely modified in the presence of strong spin–orbit coupling (Hikami *et al* 1980), giving rise to so-called weak-anti-localisation (WAL). As shown in several experiments, most notably those of Bergmann (1982a, b, c), WL and WAL both provide an excellent probe for the determination of system parameters such as the scattering relaxation times.

Several groups have studied polycrystalline bismuth films. Earlier work includes that of Komnik *et al* (1982), McLachlin (1983), Woerlee *et al* (1983) and McLachlan and White (1984), while more recently Koike *et al* (1985) and Komori *et al* (1987) have done measurements on granular bismuth/bismuth oxide films. The earlier work showed that the T and B dependence of σ of thin polycrystalline bismuth films could be ascribed to a combination of 2D WAL and 2D EEI. Koike *et al* (1985) measured thicker (3D) granular bismuth films and found that the conductivity and magnetoconductivity arose from a

† Present address: Department of Physics, University of Southern California, Los Angeles, CA 90089, USA.

0953-8984/89/376665 + 13 $02.50 © 1989 IOP Publishing Ltd

combination of 3D WAL and 3D EEI. A specific study of the temperature dependence of the inelastic scattering length was done by both Koike *et al* (1985) and Komori *et al* (1987), who found that the temperature dependence of the conductivity below 5 K in more highly disordered bismuth/bismuth oxide films is apparently stronger than the usually observed 2D (ln T) or 3D (T) and EEI dependences. Koike *et al* (1985) ascribed this stronger temperature dependence to the onset of strong localisation.

This particular work originated from the observation of an apparent lack of repeatability in the transport properties of films sputtered onto substrates held at ambient temperature, indicating that a crossover between different film characteristics occurs at substrate temperatures of around 20–25 °C. In this paper it is shown that it is possible to vary the crystalline orientation relative to the substrate in polycrystalline bismuth films by argon ion beam sputtering the films onto glass substrates held at different temperatures (−78, 0 and 50 °C). The 50 °C films (the abbreviation '50 °C film' implies that the film was sputtered onto a substrate held at 50 °C) show the usual smooth characteristic WAL temperature dependence below 15 K. On the contrary, the −78 °C films and 0 °C films show a more complex temperature dependence, with a change in the temperature dependence of the resistivity occurring between 3 and 4 K. This observation is similar to that in the more highly resistive granular bismuth/bismuth oxide films of Koike *et al* (1985) and Komori (1987).

The magnetoresistance of all the films is well described by WAL, permitting the calculation of scattering times and/or lengths using the theories of Fukuyama and Hoshino (1981) in 2D and Maekawa and Fukuyama (1981) in 3D. A deviation from the typical WAL and EEI temperature dependences is observed at the lowest temperatures in the 0 °C films and −78 °C films. An analysis of the magnetoresistance results shows that this is probably caused by a change in the exponent ($p/2$) of the inelastic scattering length between 3 and 4 K ($L_{in} = L_{in}/T^{p/2}$). Similar results, reported by Koike *et al* (1985), were interpreted to have arisen because of the onset of strong localisation.

2. Theory

As all the films were found to lie in the WL regime below 15 K the theoretical expressions for the T and B dependences of the resistivity arising from WAL and EEI are presented here. A number of researchers, using different approaches, have calculated the conductivity corrections arising from WL and WAL. The temperature dependence was calculated by Abrahams *et al* (1979) and Gorkov *et al* (1979) for the 2D case, and by Kawabata (1980) and Kaveh and Mott (1982a, b) for the 3D case. The correction resulting from strong spin–orbit coupling to WL (which gives rise to WAL) was given by Hikami *et al* (1980). Altshuler and Aronov (1979a, b), Altshuler *et al* (1980a, b) and Fukuyama (1980, 1981a, b) give the EEI expressions for both 2D and 3D .

The temperature dependences of the resistivity $R(T)$, normalised with respect to $R(T_0)$ ($T_0 = 4$ K in this work) in 2D, are given by (with $\Delta R(T)/R(T) \equiv [R(T) - R(T_0)]/R(T_0)$)

$$\Delta R(T)/R(T_0) = +(e^2/2\pi^2\hbar)R(T_0)p \ln(T/T_0) \tag{1a}$$

for WAL and

$$\Delta R(T)/R(T_0) = -(e^2/2\pi^2\hbar)R(T_0)g_2(\text{lo or hi}) \ln(T/T_0) \tag{1b}$$

for EEI. WAL is suppressed by high magnetic fields B, when $L_B = \sqrt{\hbar/eB} < L_{in}$ (see,

e.g., Bergmann 1983) in both 2D and 3D. g_2(lo or hi) is defined as *some* combination of the EEI interaction constants g_i ($i = 1, 2, 3, 4$) as described by Fukuyama (1983). As a consequence of the complicated Fermi surface and the possibility of inter-valley scattering, coupled with the high spin–orbit interaction strength in bismuth, a precise definition of g_2 is impossible. g_2(lo) and g_2(hi) are applicable in zero field and high fields, respectively. The high-field condition for EEI is $L_B = \sqrt{\hbar/eB} < L_T = \sqrt{\hbar D/kT}$ (Fukuyama 1983), where D is the diffusion constant and k is the Boltzmann constant.

In 3D the temperature dependences arising from WAL and EEI are given by

$$\Delta R(T)/R(T_0) = +(e^2/2\pi^2\hbar)R(T_0)T^{p/2}/2L_{\text{in}}(1\ K) \tag{2a}$$

$$\Delta R(T)/R(T_0) = -(e^2/2\pi^2\hbar)R(T_0)g_3(\text{lo or hi})\sqrt{kT/\hbar D}. \tag{2b}$$

Here g_3(lo or hi) is again a combination of the EEI interaction constants as defined by Fukuyama (1983). The inelastic diffusion length L_{in} is related to the inelastic scattering time τ_{in} by $L_{\text{in}} = \sqrt{D\tau_{\text{in}}}$, where $D = v_F^2\tau_0/3$ is the diffusion constant, τ_0 is the elastic scattering relaxation time and v_F is the Fermi velocity. Equations (1*a*) and 2*a*) are written for the specific case where the temperature dependence of the inelastic length is given by

$$L_{\text{in}} = L_{\text{in}}(1\ \text{K})/T^{p/2}. \tag{3}$$

It is found that $L_{\text{in}}(1\ \text{K})$ is dependent on substrate temperature T_s during sputtering, and $p/2$ depends on both T and T_s. For WL without spin–orbit coupling (Hikami *et al* 1980), the pre-factor $e^2/2\pi^2\hbar$ in equations (1*a*) and (2*a*) is replaced by $-e/\pi^2\hbar$. These equations will be referred to as equations (1*a*′) and (2*a*′).

The dimensionality of the films (for film thickness d) is determined by the following:

$L_{\text{in}} > d$	for 2D
$L_{\text{in}} < d$	for 3D WAL
$L_T > d$	for 2D
$L_T < d$	for 3D EEI.

The positive magnetoresistance arising from WAL in a field B perpendicular to the films is given by the theory of Fukuyama and Hoshino (1981) in 2D and Maekawa and Fukuyama (1981) in 3D. Defining $\Delta R(B)/R_0 = [R(B,T) - R(0,T)]/R(0,T)$, the magnetoresistance in 2D is given by

$$\begin{aligned}\Delta R(B)/R_0 = (e^2/2\pi^2\hbar)R(0,T)[\![&\psi(\tfrac{1}{2} + 1/\alpha BL_0^2) - \psi(\tfrac{1}{2} + 1/\alpha BL_{\text{S-O}}^2) - 1/2\sqrt{1-\gamma}\\ &\times \{\psi[\tfrac{1}{2} + (2/\alpha BL_{\text{S-O}}^2)(1+\sqrt{1-\gamma})] - \psi[\tfrac{1}{2} + 1/\alpha BL_{\text{in}}^2 + (2/\alpha BL_{\text{S-O}}^2)\\ &\times (1-\sqrt{1-\gamma})]\} - \ln(L_{\text{S-O}}^2/4L_0^2) + \tfrac{1}{2}\ln(L_{\text{S-O}}^2/12L_{\text{in}}^2)]\!].\end{aligned} \tag{4a}$$

For 3D films the magnetoresistance is given by

$$\begin{aligned}\Delta R(B)/R_0 = \{&\sqrt{h}F(1+t/h) + \tfrac{1}{2}\sqrt{h/(1-\gamma)}[F(t_+/h) - F(t_-/h)]\\ &- \sqrt{t_- + t_+}/\sqrt{1-\gamma} + \sqrt{t} - \sqrt{t+1}\}\\ &\times [(8/3\sqrt{3})(E_F\tau_0/\hbar)^2(L_{\text{S-O}}/L_0) + 3\sqrt{t+1} - \sqrt{t}]^{-1}\end{aligned} \tag{4b}$$

where $L_{\text{S-O}}$, L_0 and L_{in} are the spin–orbit length, elastic length and inelastic diffusion length, respectively. The respective scattering lengths and times are related by $L_x = \sqrt{D\tau_x}$ where D is the diffusion constant.

The function F is defined by

$$F(x) = \sum_{N=0}^{\infty} \left[2\left(\sqrt{N+1+1/x} - \sqrt{N+1/x}\right) - \frac{1}{\sqrt{N+\frac{1}{2}+1/x}} \right]. \qquad (4c)$$

A non-linear least-squares computer program was used to fit the theoretical expressions (4*a*) and (4*b*) to the experimental data using $L_{\text{S-O}}$, L_{in} and $E_F\tau_0/\hbar$ as parameters. Expressions (4*a*) and (4*b*) are insensitive to values of L_0 of order 3 nm, and hence another method had to be found to determine L_0. This was done as follows. The carrier concentration n is usually related to the Hall coefficient by the well known expression (see, e.g., Ashcroft and Mermin 1976):

$$R_H = 1/ne. \qquad (5)$$

Although the films are a complicated polycrystalline two-carrier system, the single-carrier expression (equation (5)) was used to obtain the carrier density to first approximation. This is because it can be shown that the more complicated two-band compensated expression (see, e.g., Busch and Schade 1976) reduces to equation (5) except for a factor of order unity, on substitution of the bulk bismuth electron and hole effective masses.

The elastic scattering length L_0 can be determined using the $T = 0$ extrapolation of the conductivity in the range 15–300 K, and the usual Boltzmann expression for the conductivity (see, e.g., Ashcroft and Mermin 1976). This gives L_0 to an accuracy of 15%, k_F being determined from the free-electron formula using the value of n obtained from the Hall coefficient.

To reduce further the number of parameters used in the computer fit, the spin–orbit scattering length and the elastic scattering length were related to each other using $L_{\text{S-O}}/L_0 = (1/\alpha Z)^2$, where $\alpha = 1/137$ and Z is the atomic number (Mersevey and Tedrow 1978). This relationship holds only to first approximation, as the spin–orbit scattering may well be enhanced in thinner films, as was found in thin copper films by Fehr *et al* (1986). Originally $L_{\text{S-O}}$ was used as an additional fitting parameter as well, but as values of order 10 nm were obtained for all the films, $L_{\text{S-O}}$ was subsequently fixed at this value. This is consistent with the value of L_0 found from the Hall coefficient and zero-temperature resistivity. The dimensionality of the films was determined by comparing $L_{\text{in}}(T)$ with d. It was found that the parameters obtained from 2D or 3D computer fits to the data were similar in the transition region.

The calculated value of the semi-classical two-band magnetoresistance (see, e.g., Busch and Schade 1976) is 0.05% at 1.5 T, independent of T. Magnetoresistance results above 12 K thus cannot be interpreted merely in terms of WAL.

3. Experimental details

Bismuth films were argon ion beam sputtered from a bismuth (purity 99.9999%) target onto flame-polished glass held at −78, 0 or 50 °C. The partial pressure of all gases other than argon was below 5×10^{-7} mbar during sputtering. Film thicknesses ranged between 20 and 200 nm and were measured (accuracy, 5%) with a calibrated vibrating-crystal thickness monitor (Inficon XTM). The slides were mounted inside the sputtering chamber on the bottom of a rotating temperature bath. Solid CO_2 in acetone, ice in water and a thermostatically controlled heated-oil bath were used to maintain the

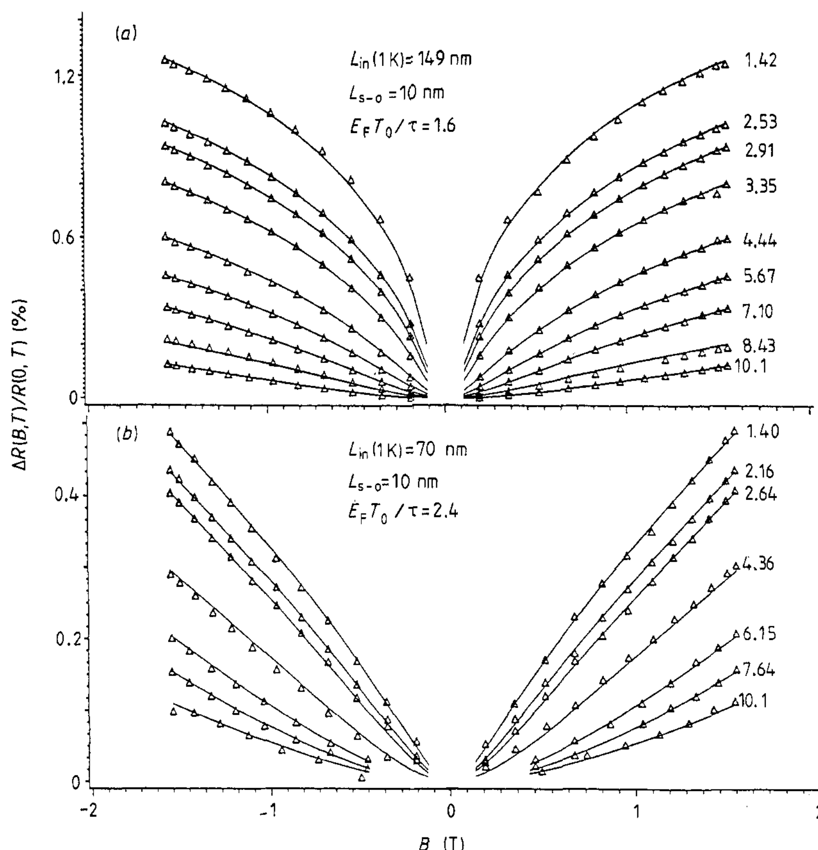

Figure 1. Magnetoresistance of (*a*) a 20 nm, 0 °C film and (*b*) a 200 nm, 0 °C film: ——, computer fit of the theory of Mackawa and Fukuyama (1981) for the 20 nm film and of Fukuyama and Hoshino (1981) for the 200 nm film. The fitting parameters are shown in the figure. A plot of L_{in} as a function of temperature as determined from the computer fitting is shown in figure 3.

respective temperatures. Gas had to be bubbled rapidly through the heated oil to mix the oil so as to ensure that the temperature was uniform throughout. Temperature drifts were smaller than 1% in the bath (and presumably on the substrate) during the sputtering period.

A HP 150 computer-controlled system, comprising a HP 3497A data aquisition–control unit and a HP 3456A DVM coupled to two lock-in amplifiers, was utilised to measure the resistance, magnetoresistance and Hall coefficient of the films between 1.4 and 273 K and in fields up to 1.5 T. A Kelvin–Varley divider bridge was used to offset approximately 90% of the sample resistance voltage, enabling a higher-sensitivity setting to be used on the lock-in amplifiers. A relative accuracy of 1 part in 10^5 was achieved for the resistance measurements, while the Hall coefficients were measured to a relative accuracy of approximately 5%. The absolute accuracy of both the resistivity and the Hall coefficient measurements was limited by inaccuracies in film thickness determination. Measurements on the films show that the resistivities of the films do not change measurably over a period of several weeks at room temperature, indicating that any annealing which might occur either is very slow or takes place within a few hours of sputtering,

Table 1. Important parameters of the films.

Thickness (nm)	Sputtering temperature (°C)	Resistivity ($\mu\Omega$ cm)		Dimensionality below 10 K
		4 K	300 K	
200	50	3.3	2.3	3D
200	0	3.9	2.8	3D
200	−78	3.2	2.6	3D
40	50	1.6	1.5	2D
40	0	1.8	1.7	2D
20	0	1.25	1.20	2D
20	−78	1.45	1.40	2D

before any measurements can be done. Previous work (Stoddart and McLachlan 1986) showed that the 0 °C bismuth films are continuous at thicknesses above 8 nm, and well out of the 2D percolation regime at 20 nm; however, the 50 °C films still show 2D percolation characteristics at 20 nm and so only the 40 nm, 50 °C films and the 200 nm, 50 °C films are studied here.

X-ray diffraction studies on the films indicate that the crystallites of the 78 °C films are oriented with predominantly the [102] axis perpendicular to the substrate, while the 50 °C films and 0 °C films are oriented with predominantly the [001] axis perpendicular to the substrate. The −78 °C films and 0 °C films also show smaller diffraction peaks, indicating the presence of crystallites oriented with the [105] and [104] axes perpendicular to the substrate. These orientations are both absent in the 50 °C films.

Samples for transmission electron microscopy were prepared by placing thin Formvar films on copper grids in the conventional way, and then sputtering 50 nm glass from a glass target, in the presence of oxygen at 1×10^{-5} mbar, onto the Formvar-covered grid. The bismuth films were sputtered onto the glass. Micrographs of the films show that the films are highly polycrystalline, with the crystallite diameter being approximately 30 nm. No obvious change in crystallite size is observed for the different substrate temperatures used during sputtering. The grain boundaries do, however, become better defined with increasing substrate temperature during sputtering.

4. Results

A summary of some important parameters of the films is given in table 1. The resistivity at 4 K is primarily dependent on the thickness of the films, with the 200 nm films having a resistivity (at 4 K) approximately twice that of the 20 nm films. Of the 20 nm films, the 0 °C film has a lower resistivity than the −78 °C film, while of the 40 nm films the 50 °C film has a lower resistivity than the 0 °C film. However, of the 200 nm films the situation is reversed with the −78 °C film having the lowest resistivity (at 4 K) and the 50 °C film having the highest resistivity. Other than the dominant dependence on thickness, there appears to be no consistent pattern in the 4 K resistivity.

All the films except the 20 nm, 0 °C film have a temperature dependence which can be approximated by a power law. The temperature dependence of the data above 15 K can be approximated by the 3D WL (weak spin–orbit coupling) expression (equation (2a')) with $p = 1.5$. This suggests that WL and EEI persist up to room temperature. The

use of WL, as opposed to WAL, is justified as a crossover between WAL and WL occurs at approximately 15 K when $L_{in}(T) \simeq L_{S\text{-}O}$ (determined from the magnetoresistance analysis). A negative magnetoresistance is not observed, however, as a consequence of the larger positive semi-classical contribution observed in 3D films at temperatures of about 15 K and above. The 20 nm, 0 °C film shows two distinct regimes of temperature dependence. Below 100 K the temperature dependence is not a power law, while above 100 K a power-law temperature dependence similar to that of the other films is observed.

The magnetoresistance of all the films, below 15 K, can be well described by the WAL theory of Fukuyama and Hoshino (1981) (equation (4*a*)) for 2D films and Maekawa and Fukuyama (1981) (equation (4*b*)) for 3D films. Examples of the magnetoresistance results and the theoretical curves obtained for the 20 nm, 0 °C and 200 nm, 0 °C films are shown in figures 1(*a*) and 1(*b*). The magnetoresistance of all the thinner films (20 and 40 nm) is well described by the 2D theory up to 15 K, while all the 200 nm films are better described by the 3D theory.

Figure 2 shows the temperature dependences of the resistivity of all the films below 15 K. In figure 2(*d*) the temperature dependence of the 40 nm, 50 °C film is seen to be logarithmic up to 7 K, both at zero field and at 1.5 T (which is explicable by a combination of 2D WAL and 2D EEI). $g(\mathrm{lo})$ and $g(\mathrm{hi})$ can be calculated from the slope of the curve of resistance against $\ln T$ using the value of p determined from the magnetoresistance measurements. For the 40 nm, 50 °C film, $g(\mathrm{lo}) = g(\mathrm{hi}) = 1.2 \pm 0.1$. The EEI contribution thus remains unchanged (within experimental error), and the magnetoresistance arises mainly from the suppression of WAL by the applied magnetic field.

The resistivity of the 20 and 40 nm films sputtered onto substrates held at −78 °C and 0 °C is not simply logarithmic in temperature at 0 T. However, at 1.5 T the temperature dependence is logarithmic (figure 3(*a*)), arising from 2D EEI (WAL being suppressed at 1.5 T).

For the 200 nm films the high-field temperature dependence is slightly more complicated because of the semi-classical B^2 magnetoresistance (0.05% at 1.5 T), but a WAL magnetoresistance analysis is still done. The B^2 contribution is absent in 2D films at low temperatures.

Three possible mechanisms suggested by Koike *et al* (1985) could give rise to the observed apparent strengthening in the temperature dependence of the resistivity for the −78 °C films and 0 °C films:

(i) the occurrence of a dimensional crossover;

(ii) one-dimensional WAL arising from a percolation network of fine 'wires' through a non-conducting base; and

(iii) the onset of a variable-range hopping channel (as pointed out by Koike *et al* (1985), variable-range hopping can give rise to a large anomalous positive contribution to the magnetoresistance: the numerical calculations of Kurobe and Kamimura (1982) are not, however, directly comparable with experiment).

The simple logarithmic temperature dependence of the resistivity in the 50 °C films compared with the −78 °C films and 0 °C films rules out the dimensionality crossover mechanism (i). The percolation mechanism (ii) can be immediately ruled out in this case owing to continuity of the films and the absence of the insulating phase in pure bismuth compared with the bismuth/bismuth oxide films of Koike *et al* (1985). Mechanism (iii), variable-range hopping, is unlikely as the magnetoresistance is well described by WAL.

There is, however, the possibility of a changeover in the dominant mechanism of the inelastic scattering. This will now be considered in detail.

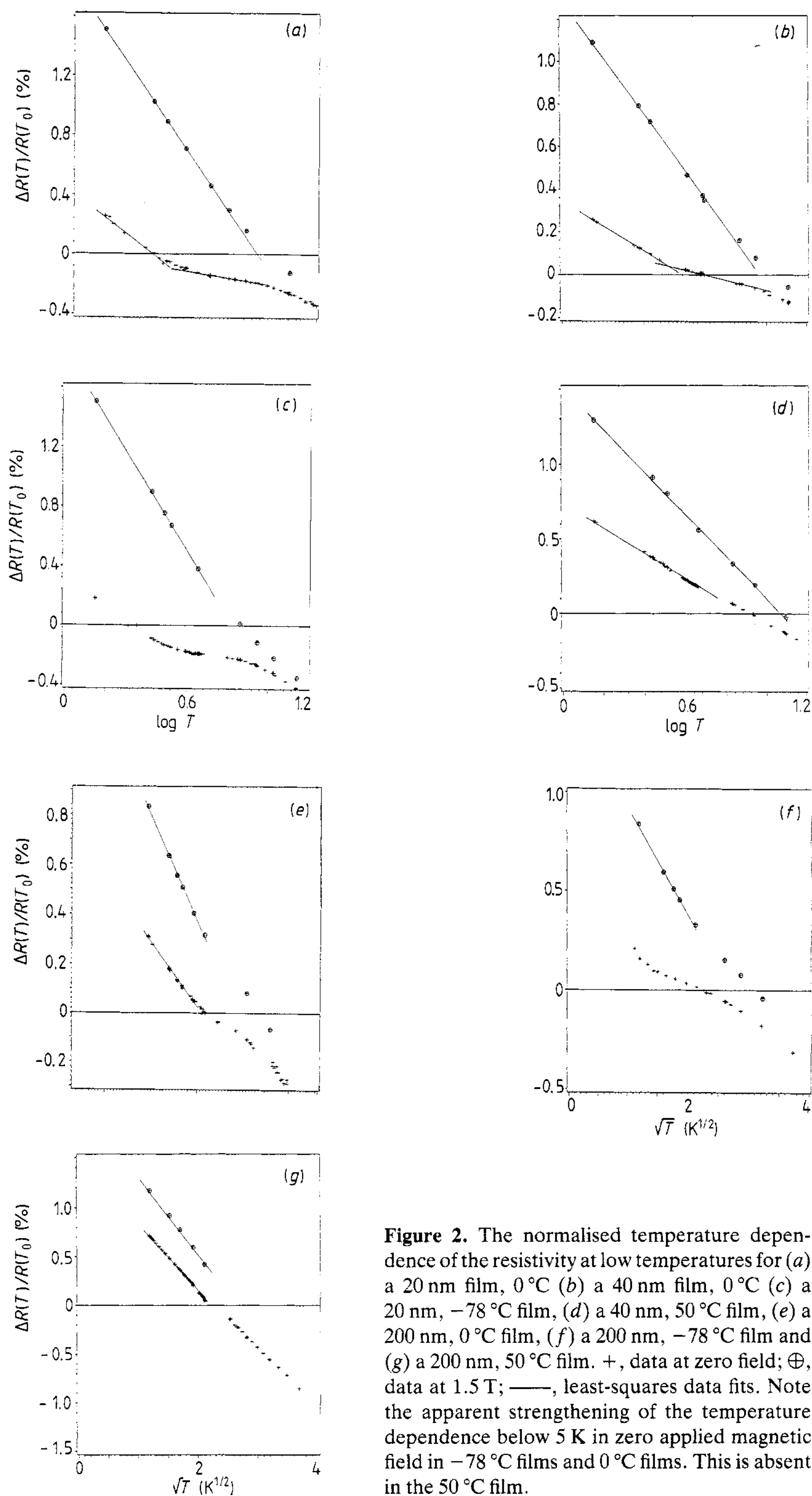

Figure 2. The normalised temperature dependence of the resistivity at low temperatures for (*a*) a 20 nm film, 0 °C (*b*) a 40 nm film, 0 °C (*c*) a 20 nm, −78 °C film, (*d*) a 40 nm, 50 °C film, (*e*) a 200 nm, 0 °C film, (*f*) a 200 nm, −78 °C film and (*g*) a 200 nm, 50 °C film. +, data at zero field; ⊕, data at 1.5 T; ——, least-squares data fits. Note the apparent strengthening of the temperature dependence below 5 K in zero applied magnetic field in −78 °C films and 0 °C films. This is absent in the 50 °C film.

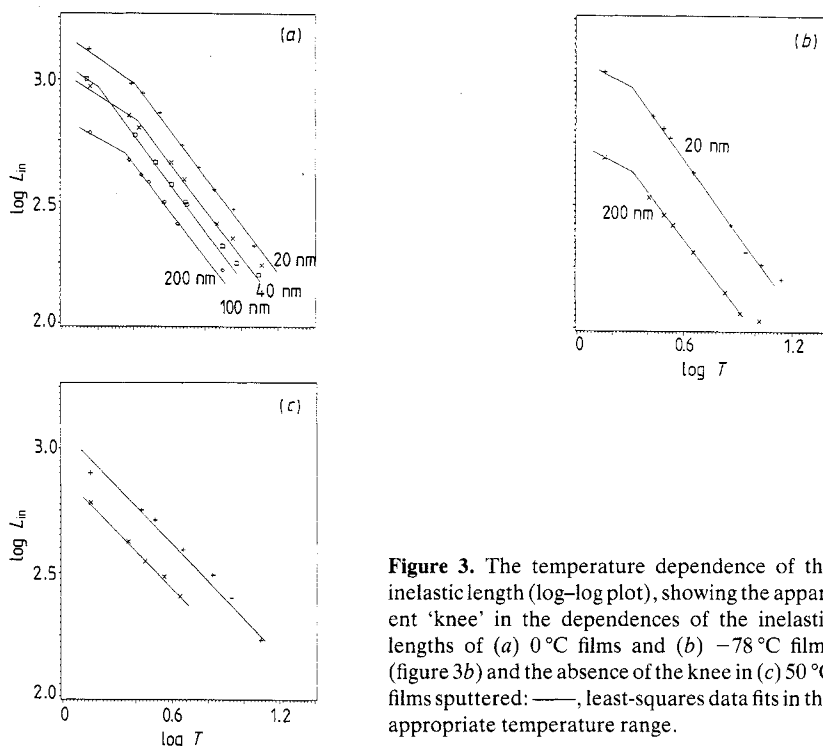

Figure 3. The temperature dependence of the inelastic length (log–log plot), showing the apparent 'knee' in the dependences of the inelastic lengths of (*a*) 0 °C films and (*b*) −78 °C films (figure 3*b*) and the absence of the knee in (*c*) 50 °C films sputtered: ——, least-squares data fits in the appropriate temperature range.

The parameters obtained from the data-fitting procedure which are used for the theoretical curves are given, for all the films, in table 2. $L_{in}(1\ K)$ is observed to decrease as the resistivity increases and the film thickness increases. The temperature dependences of the various inelastic lengths are shown in figure 3. The most puzzling feature is the 'knee' in the temperature dependence of L_{in} for the −78 °C films and 0 °C films. No knee is observed in the temperature dependence of L_{in} for the 50 °C films.

The exponent $p/2$ of the temperature dependence of L_{in} (equation (3)) is obtained from the slope of the log–log plot of the inelastic length against temperature (figure 3). As the theories all predict integral or half-integral values for p, rather than carrying out a least-squares fit to determine the slope, the slopes were *chosen* to be 0.5, 0.75, 1 or 1.5, depending on which gave the best fit to the data. This method was found to yield unambiguous values for $p/2$. For the 50 °C films, $p/2 = 0.75$ below 15 K with $L_{in} \simeq$ 100 nm. The −78 °C films and 0 °C films show a $p/2 = 0.5$ dependence at the lowest temperatures, with a crossover to $p/2 = 1.0$ occurring at 2.6–3.0 K.

Altshuler (1982) calculated the temperature dependence of L_{in} due to electron-electron scattering. This gives $p/2 = 0.5$ and can be written

$$L_{in} = \surd(2D/kT)(m^*/3)[v_F d/\ln(v_F d m^*/3\hbar)] \qquad (6)$$

where m^* is the carrier effective mass, v_F is the Fermi velocity and d is the thickness of the film. Using the parameters in table 2, this expression predicts that $L_{in}(1\ K)$ is 120 nm (for holes) and 380 nm (for electrons) for the 20 nm film, and 210 nm (for holes) and 670 nm (for electrons) for the 200 nm film. Although these values of $L_{in}(1\ K)$ are of the correct order of magnitude, the thickness dependence is incorrect in this case. No explanation for this discrepancy could be found.

Table 2. Derived parameters of the bismuth films. $L_{in}(1\ K)$, $p/2$ and $E_F\tau_0/\hbar$ were determined from computer fits of the magnetoresistance expressions (equations 4(*a*) and 4(*b*)) to the data. Two different values of $L_{in}(1\ K)$ and $p/2$ are quoted for the 78 °C films and the 0 °C films; $p/2=\frac{1}{2}$ and $p/2=1$ correspond to the temperature ranges below and above approximately 3 K (see figure 3). n was obtained from the Hall coefficient (equation (5)) and L_0 was obtained from the Boltzmann conductivity.

Sample sputtering temperature (°C)	Thickness (nm)	$L_{in}(1\ K)$ (nm)	$p/2$	$E_F\tau_0/\hbar$	(10^{20} cm^3)	L_0 (nm)
0	20	149	0.5	1.6	7.7	1.5
0	20	243	1	1.6	7.7	1.5
0	40	107	0.5	2.0	3.6	2.0
0	40	184	1	2.0	3.6	2.0
0	200	70	0.5	2.4	0.8	2.4
0	200	122	1	2.4	0.8	2.4
−78	20	118	0.5	2.8	—	1.5
−78	20	190	1	2.8	—	1.5
−78	200	59	0.5	1.2	—	2.5
−78	200	89	1	1.2	—	2.5
50	40	116	0.75	1.8	2.0	2.1
50	200	77	0.75	1.6	1.1	2.7

Although it is not strictly a $p=1$ process, the Abrahams *et al* (1981) mechanism predicts that

$$\tau_{in}=(E_F\tau_0/kT)[1/\ln(T_1/T)]$$

where

$$T_1=(\hbar/k)(D\varepsilon^2\varepsilon_0^2/l^4).$$

Here $\varepsilon_0=8.85\times10^{-12}\ \mathrm{F\ m^{-1}}$ is the permittivity constant, $\varepsilon=Dh/l_s$ is the dielectric constant (with l_s being the Thomas–Fermi screening length). In the limit $T_1\gg T$, which can be shown to be true in bismuth films below 15 K, this process does, however, give rise to an effective $p=1$ process.

For the 20 nm films, this process predicts that $L_{in}(1\ K)=39$ nm for holes and $L_{in}(1\ K)=81$ nm for electrons. For the 200 nm films, we find that $L_{in}(1\ K)=46$ nm and 84 nm for holes and electrons, respectively. This process thus predicts values of $L_{in}(1\ K)$ of the correct order of magnitude, but the calculated values are almost independent of thickness, which is not what is observed.

Several mechanisms could cause the $p/2=1$ dependence observed at temperatures above the crossover from $p/2=\frac{1}{2}$. The first is Landau–Baber electron–electron scattering in disordered materials (see, e.g., Kaveh and Wiser 1984, Bronovoi and Sharvin 1978). This gives rise to the following expression for L_{in}:

$$L_{in}=\sqrt{hD/2\pi k^2a^3N(E_F)}\,(1/T) \qquad (7)$$

where $N(E_F)$ is the density of states at the Fermi level. Using the free-electron value for $N(E_F)$ calculated using the carrier densities given in table 2, and $a=0.2$ nm (a is the approximate distance between nearest-neighbour bismuth atoms), this gives values of $L_{in}(1\ K)$ varying from 8500 to 12 500 nm with increasing film thickness. These values are

an order of magnitude greater than those observed and again have the incorrect thickness dependence.

The second possibility is the electron–phonon scattering mechanism of Bergmann (1982c), which gives

$$L_{in} = (L/n)\sqrt{Mm^* L_0 c^3 D}\,(1/kT) \tag{8}$$

where $L = 2{\cdot}8 \times 10^{22}\,\mathrm{cm}^{-3}$ is the number of bismuth atoms per cubic centimetre, n is the electron density, M is the ion mass, $L_0 = 3$ nm is the elastic scattering length determined from magnetoresistance measurements and c is the speed of sound in bismuth which is typically $3 \times 10^4\,\mathrm{m\,s^{-1}}$ in a metal (see, e.g., Weast 1981). At 1 K this mechanism predicts an inelastic length of typically 10^4 nm, increasing with increasing thickness.

The third possible $1/T$ mechanism, suggested by Takayama (1973), also arises from electron–phonon scattering. This can be written

$$L_{in} = [D(E_F\tau_0/\hbar)/2\pi^2\lambda]\sqrt{\hbar/k\theta_D}\,(\theta_D/T). \tag{9}$$

Here $\theta_D \simeq 118$ K is the Debye temperature for bismuth (Weast 1981), and $E_F\tau_0/k \simeq 2$ (from the magnetoresistance measurements). λ is defined

$$\lambda = nmv_F^2 q_0^2/6LMc^2k_F^2$$

where q_0 is related to the Debye temperature by $q_0 = k\theta_D/\hbar c$. This process gives $L_{in}(1\,\mathrm{K})$ of order 500 nm, again increasing with increasing thickness. In summary it is seen that all three mechanisms for the $p/2 = 1$ dependence thus overestimate $L_{in}(1\,\mathrm{K})$ quite markedly.

The $p/2 = 0.75$ dependence observed for the 50 °C films is more amenable to theoretical description. Schmid (1974) proposed the following temperature dependence for τ_{in}:

$$\tau_{in} = (8/\pi)[(\hbar E_F/kT)^2][1 + (4\sqrt{3}/\pi)(\hbar/E_F\tau_0)^{3/2}\sqrt{E_F/kT}]^{-1}. \tag{10a}$$

The term $(4\sqrt{3}/\pi)(\hbar/E_F\tau_0)^{3/2}$ is much larger than unity (using the parameters in table 2) and hence can be approximated by

$$L_{in} = (2D/3)(E_F\tau_0/\hbar)^{3/2}\hbar\sqrt{E_F}(1/kT)^{3/2}. \tag{10b}$$

This gives $p/2 = 0.75$, with $L_{in}(1\,\mathrm{K}) = 471$ nm and 2600 nm for holes and electrons, respectively, for the thinnest film and $L_{in}(1\,\mathrm{K}) = 323$ nm and 1820 nm for holes and electrons, respectively, for the thickest film. These values can be compared with the values obtained from the magnetoresistance analysis of 181 nm for the 40 nm film and 141 nm for the 200 nm film. Thus, even though the Schmid process overestimates the absolute value of the inelastic length, by a factor of 3 or 4, it is not in conflict with the implicit thickness dependence.

5. Conclusions

In conclusion, the observed change in the temperature dependence of the resistivity at low temperatures presumably arises from a changeover in the predominant scattering at approximately 3 K in the −78 °C and 0 °C films. In order to understand the origin of this crossover consider the following points.

(i) The crystalline size is unchanged by different substrate temperatures during sputtering, and therefore this and a resulting change in L_0 is ruled out as a possible cause.

(ii) The predominant crystallite orientation perpendicular to the substrate is different in the −78 °C film ([102]) from that in the 0 °C films and 50 °C films which have a predominant crystallite orientation of [001]. This rules out the possibility that the predominant crystallite orientation causes the observed temperature dependence.

(iii) A possible cause of the different scattering mechanisms in the −78 °C films and 0 °C films compared with the 50 °C films is then the presence of crystallites of orientation [014] and [105] in the −78 °C films and 0 °C films. These orientations are absent in the 50 °C films. The presence of these crystallites could affect the temperature dependence in two ways.

(*a*) The increased mismatch between crystallites due to the occurrence of crystallites of several different orientations, could enhance the scattering at the grain boundaries.

(*b*) The second possibility is that the mechanism of scattering is dependent on the orientation of the crystallites, with Schmid electron scattering dominating in [001] crystallites, while the observed $p/2 = 1$ scattering dominates in [104] and [105] crystallites.

The predominant inelastic scattering mechanism in sputtered bismuth films is thus probably dependent on the microscopic structure of the films. Some existing models for the temperature dependence of the inelastic length predict values of the correct order of magnitude. However, the thickness dependence of the inelastic length in the −78 °C films and 0 °C films is at variance with the available models. It is possible, however, that spin–orbit coupling may have a direct influence on the inelastic length. Spin–orbit coupling is not taken into account in the models.

Acknowledgments

The authors wish to thank F R L Schoening and J Salemi for the x-ray diffraction work, as well as the electron microscope unit of the University of the Witwatersrand. The technical assistance of Dominic Mqoco is also greatly appreciated.

References

Abrahams E, Anderson P W, Lee P A and Ramakrishnan T V 1981 *Phys. Rev.* B **24** 6783
Abrahams E, Anderson P W, Licciardello D C and Ramakrishnan T V 1979 *Phys. Rev. Lett.* **42** 673
Altshuler B L 1982 *J. Phys. C: Solid State Phys.* **15** 7367
Altshuler B L and Aronov A G 1979a *Solid State Commun.* **30** 115
—— 1979b *Zh. Eksp. Teor. Fiz.* **77** 2028 (Engl. Transl. 1979 *Sov. Phys.–JETP* **50** 968)
Altshuler B L, Aronov A G and Lee P A 1980a *Phys. Rev. Lett.* **44** 1288
Altshuler B L, Khmel'nitzkii D, Larkin A I and Lee P A 1980b *Phys. Rev.* B **22** 5142
Ashcroft N W and Mermin N D 1976 *Solid State Physics* (Saunders College, PA: Holt, Rinehart and Winston)
Bergman G 1982a *Phys. Rev. Lett.* **49** 162
—— 1982b *Phys. Rev. Lett.* **48** 1046
—— 1982c *Z. Phys.* B **48** 5
—— 1983 *Phys. Rev.* B **28** 2914
Bronovoi I L and Sharvin Y V 1978 *JETP Lett.* **28** 117
Busch G and Schade H 1976 *Lectures on Solid State Physics, International Series in Natural Philosophy* vol 79 (Oxford: Pergamon)

Fehr Y, May-Tal S and Rosenbaun R 1986 *Phys. Rev.* B **33** 6631
Fukuyama H 1980 *J. Phys. Soc. Japan* **48** 2169
—— 1981a *J. Phys. Soc. Japan* **50** 3407
—— 1981b *J. Phys. Soc. Japan* **50** 3562
—— 1983 *Institute of Solid State Physics, University of Tokyo, Technical Report, Ser A,* 1304
Fukuyama H and Hoshino K 1981 *J. Phys. Soc. Japan* **50** 2131
Gorkov L P, Larkin A I and Khmelnitskii D E 1979 *JETP Lett.* **30** 228
Hikami S, Larkin A L and Nagaoka Y 1980 *Prog. Theor. Phys.* **63** 707
Kaveh M and Mott N F 1982a *J. Phys. C: Solid State Phys.* **15** L697
—— 1982b *J. Phys. C: Solid State Phys.* **15** L707
Kaveh M and Wiser N 1984 *Adv. Phys.* **33** 257
Kawabata A 1980 *Solid State Commun.* **38** 823
Koike Y, Okamura M and Fukase T 1985 *J. Phys. Soc. Japan* **54** 3018
Komnik Y F, Bukhstab E I, Butenko A V and Andrievsky V V 1982 *Solid State Commun.* **44** 865
Komori F, Okuma S and Kobayashi S 1987 *J. Phys. Soc. Japan* **56** 691
Kurobe A and Kamimura H 1982 *J. Phys. Soc. Japan* **51** 1904
Mclachlan D S 1983 *Phys. Rev.* B **28** 12 6821
McLachlan D S and White H 1984 *Proc. LITPIM Suppl.* PTB-PG-1, PTB Braunschweig
Maekawa S and Fukuyama H 1981 *J. Phys. Soc. Japan* **50** 2516
Mersevey R and Tedrow P M 1978 *Phys. Rev. Lett.* **41** 805
Schmid A 1974 *Z. Phys.* **271** 251
Stoddart S and McLachlan D S student project, unpublished
Takayama H 1973 *Z. Phys.* **262** 329
Weast R C (ed.) 1981 *CRS Handbook of Chemistry and Physics* 62nd edn (West Palm Beach, FL; CRC Press)
Woerlee P H, Verkade G C and Jansen A G M 1983 *J. Phys. C: Solid State Phys.* **16** 3011